AMERICAN ACADEMY OF OPHTHALMOLOGY®

Multimodal Imaging and *En Face* OCT Detection of Calcified Drusen in Eyes with Age-Related Macular Degeneration

Jeremy Liu, BS,[1] *Rita Laiginhas, MD,*[1] *Mengxi Shen, MD,*[1] *Yingying Shi, MD,*[1] *Jianqing Li, MD,*[1] *Omer Trivizki, MD,*[1] *Nadia K. Waheed, MD,*[2] *Giovanni Gregori, PhD,*[1] *Philip J. Rosenfeld, MD, PhD*[1]

Purpose: *En face* OCT imaging was investigated as a method for the detection and monitoring of calcified drusen in eyes with nonexudative age-related macular degeneration (AMD).

Design: Retrospective case series of a prospective study.

Participants: Patients with nonexudative AMD.

Methods: A retrospective review was performed of same-day color fundus (CF), fundus autofluorescence (FAF), near-infrared (NIR), and *en face* swept-source (SS) OCT images to identify eyes with nonexudative AMD and calcified drusen. The appearance and progression of these lesions were compared using the different imaging methods.

Main Outcome Measures: Comparison between the presence of calcified drusen observed on CF images with the detection of these lesions on FAF, NIR, and *en face* SS OCT images.

Results: Two hundred twenty eyes from 139 patients with nonexudative AMD were studied, with 42.7% of eyes containing calcified drusen either at baseline or during follow-up visits. On the *en face* SS OCT images, calcified drusen appeared as dark focal lesions referred to as choroidal hypotransmission defects (hypoTDs) that were detected in the choroid using a sub−retinal pigment epithelium (RPE) slab. The corresponding B-scans showed drusen with heterogenous internal reflectivity, hyporeflective cores, and hyperreflective caps. In most calcified drusen, choroidal hypertransmission defects (hyperTDs) were observed to develop over time around the periphery of the hypoTDs, giving them the appearance of a donut lesion on the *en face* SS OCT images. These donut lesions were associated with significant attenuation of the overlying retina, and the corresponding FAF images showed hypoautofluorescence at the location of these lesions. The donut lesions fulfilled the requirement for a persistent hyperTD, which is synonymous with complete RPE and outer retinal atrophy (cRORA). Six eyes displayed regression of the calcified drusen without cRORA developing. B-scans at the location of these regressed calcified drusen showed deposits along the RPE, with outer retinal thinning in the regions where the calcified lesions previously existed.

Conclusions: *En face* OCT imaging is a useful method for the detection and monitoring of calcified drusen and can be used to document the evolution of these drusen as they form donut lesions or foci of cRORA.

Drusen are the hallmark feature of intermediate age-related macular degeneration (AMD) and are characterized by focal extracellular deposits between the retinal pigment epithelium (RPE) and Bruch's membrane.[1−3] In the Age-Related Eye Disease Study, large confluent drusen were shown to be a high-risk feature for the progression to late AMD, and especially for the development of geographic atrophy (GA).[4] Later, Ouyang et al[5] performed a longitudinal study using spectral-domain OCT and showed that drusen with a heterogenous internal reflectivity were consistently found to be predictive for the onset of local atrophy. Similarly, Bonnet et al[6] conducted a retrospective case series using multimodal imaging, including spectral-domain OCT, and observed that drusen with distinctive hyperreflective pyramidal or dome-shaped structures were present in areas of GA. They termed these lesions *ghost drusen* because these structures were in regions of atrophy. In addition, Suzuki et al[7] reported on the multimodal imaging and histologic appearance of these atypical drusen and referred to them as *refractile drusen*. They proposed that these refractile drusen represented a stage of drusen regression marked by the loss of RPE as these lesions progressed to GA, and they attributed their glistening appearance to the presence of calcium-containing spherules. However, these previous studies did not identify the types of lesions that preceded the formation of these refractile drusen or the OCT characteristics of how they progressed to GA.

Tan et al[8] performed a histologic study on these drusen with heterogenous internal reflectivity and hyperreflective pyramidal structures and confirmed that the lesions contained nodules that consisted mostly of crystalline

https://doi.org/10.1016/j.xops.2022.100162
ISSN 2666-9145/22

calcium phosphate deposits. They called these deposits *calcific nodules*. In addition to the histologic findings, they conducted a longitudinal observation study using multimodal imaging that included color fundus (CF), fundus autofluorescence (FAF), near infrared (NIR), and spectral-domain OCT imaging. From this study, they found that these calcific nodules were significantly and independently associated with progression to late AMD, which included both the formation of GA and macular neovascularization. In addition, they described calcified drusen as having a hyperreflective cap along with a heterogenous internal reflectivity or hyporeflective core on OCT B-scans. Other studies have found similar results, with the Classification of Atrophy Meetings group recognizing calcified drusen as clinically significant lesions that have a high association with GA developing, which is also known as complete RPE and outer retinal atrophy (cRORA).[9–13]

Because of the irreversible loss of vision wherever cRORA is located, we wanted to understand how best to detect and observe drusen using different imaging methods as they develop these calcific properties and progress to atrophy. This is particularly important when identifying patients at high risk of disease progression and for designing clinical trials to test novel therapies that may slow the progression or prevent the formation of cRORA.[14–16] Although CF imaging is considered the gold standard for the diagnosis of calcified drusen in AMD, more recent imaging technologies, such as FAF, NIR, and OCT imaging, have advanced our understanding of AMD. These other imaging methods have several advantages compared with CF imaging, including the ability to detect lesions using different optical properties of the tissue that may result in enhanced contrast detection and may be less influenced by media opacities such as cataracts. In particular, OCT imaging can provide depth-resolved information and can localize specific anatomic changes through cross-sectional B-scan imaging. As a result, the Classification of Atrophy Meetings group recommended OCT as the reference method for defining different stages of atrophy.[13,17]

Although the characteristics and progression of calcified drusen have been described using OCT B-scans,[5–12] we used both B-scans and *en face* OCT imaging to diagnose and observe the progression of drusen in AMD.[18–24] To date, no reports have described the characteristic features of calcified drusen using an *en face* OCT imaging approach. Compared with the laborious process of reviewing each B-scan, the *en face* OCT imaging strategy allows the reviewer to look at the entire volumetric scan at a glance, which is similar to viewing the fundus on slit-lamp biomicroscopic examinations and on CF, FAF, and NIR images. As a result, *en face* OCT images can be easily compared with the appearance of fundus lesions when using different imaging methods. Moreover, *en face* imaging allows for the visualization of different anatomic layers by selecting boundary-specific slabs and reviewing selected B-scans that correspond to abnormalities detected on these slab-specific *en face* images.

In previous studies, we used a sub-RPE slab positioned from 64 to 400 μm under Bruch's membrane to obtain *en face* OCT images to identify persistent hypertransmission defects (hyperTDs) that corresponded to cRORA or GA.[25–27] These persistent hyperTDs appeared as bright areas on the *en face* OCT image because of increased light transmission into the choroid where the RPE was absent or attenuated. While studying eyes with choroidal hyperTDs, we also identified dark foci that were the result of the hypotransmission of light into the choroid, which we referred to as *choroidal hypotransmission defects* (hypoTDs). These hypoTDs are caused by any overlying structure that attenuates or scatters the incident light such as intraretinal hyperreflective foci, a thickened RPE layer, vitelliform material, blood, a large retinal pigment epithelial detachment, and calcified drusen.[28] As soon as these foci are identified on the *en face* OCT image, the cause of any hypoTDs can then be easily revealed by reviewing the corresponding B-scans. In this current case series, we used *en face* OCT and other imaging methods to study eyes with nonexudative AMD with the goal of identifying and following the progression of hypoTDs associated with calcified drusen.

Methods

This retrospective case series of a prospective study was conducted at the Bascom Palmer Eye Institute. The imaging data used in this report were from patients enrolled in an ongoing prospective swept-source (SS) OCT imaging study investigating the natural history of nonexudative AMD. The patients enrolled in this study underwent SS OCT imaging every 3 months. In addition, each patient underwent CF, FAF, and NIR imaging on a yearly basis. The institutional review board of the University of Miami Miller School of Medicine approved the study, and all patients signed an informed consent. The study was performed in accordance with the tenets of the Declaration of Helsinki and complied with the Health Insurance Portability and Accountability Act of 1996.

A retrospective review of all CF, FAF, NIR, and SS OCT images obtained from June 2016 through November 2021 was performed to identify calcified drusen in eyes with nonexudative AMD. Exclusion criteria included eyes with a history of exudative AMD, presence of diabetic retinopathy, and poor retinal image quality. Two graders (J.L. and R.L.) independently evaluated all *en face* images for the presence of calcified drusen and confirmed their gradings with the corresponding OCT B-scans, as well as the CF, NIR, and FAF images. Consensus gradings for the presence of calcified drusen were reached between the 2 graders in each eye, and any remaining disagreement was adjudicated by a senior grader (P.J.R.), who also confirmed the consensus gradings.

Imaging Protocols

Each patient underwent CF imaging using a 50° field-of-view centered on the fovea (TRC-50DX; Topcon Medical Systems). At the same visit, the patient also underwent FAF imaging (30° field-of-view centered on the fovea; HRA-II [Heidelberg Engineering]), NIR imaging (30° field-of-view centered on the fovea; HRA-II), and SS OCT angiography imaging (PLEX Elite 9000; Carl Zeiss Meditec). The SS OCT angiography instrument had a central wavelength of 1050 nm and a scanning rate of 100 000 A-scans per second. In addition, only images with a 6 × 6-mm scan pattern centered on the fovea were used in this study. This scan pattern consisted of 500 A-scans per B-scan, with each B-scan repeated twice at each position. Five hundred B-scan positions were along the slow axis, resulting in a uniform spacing of 12 μm

between A-scans and B-scans. The images were reviewed for quality and signal strength. Scans with a signal strength of < 7 based on the instrument's output and those with significant motion artifacts were excluded.

SS OCT Image Processing

The SS OCT 6 × 6-mm volume scans were used to generate *en face* structural images that were created using a sub-RPE slab positioned from 64 to 400 μm under Bruch's membrane. This *en face* structural image allowed for the detection of 2 features: (1) choroidal hyperTDs and (2) choroidal hypoTDs. On the *en face* images, hyperTDs appeared as bright areas that represented regions where increased light transmission into the choroid was present as a result of the RPE being absent or attenuated.[25–27] In contrast, choroidal hypoTDs appeared as dark focal areas on the *en face* structural image because choroidal light transmission was decreased as a result of the presence of overlying material that attenuated or scattered both the incident and reflected light. As a result, a decreased or absent signal compared with the surrounding tissue was detected by the SS OCT instrument. As previously mentioned, the main causes of hypoTDs in eyes with AMD include hyperpigmentation, blood, large pigment epithelial detachments, vitelliform lesions, and calcified drusen.

All the *en face* images for each patient were evaluated for the presence of focal hypoTDs, with the CF images serving as the reference for the detection of calcified drusen. To identify the cause of the focal hypoTDs, the corresponding B-scans were inspected and displayed calcified drusen appearing as elevations of the RPE with a heterogenous internal reflectivity or hyporeflective core along with a hyperreflective cap and choroidal hypotransmission beneath the drusen. The areas of hypoTDs on the *en face* image were also closely associated with areas of choroidal hyperTDs, and these lesions were followed up over time.

In addition to the *en face* structural images, a drusen volume map was obtained using the Advanced RPE Analysis algorithm. This is an instrument algorithm that has been validated and provides a color-coded map along with measurements of drusen volume and area.[29]

All images, including CF, FAF, NIR, and *en face* SS OCT structural scans, were exported as JPEG files and registered and resized manually using Adobe Photoshop (Adobe, Inc.). The retinal vessels were used as landmarks for the manual registration and allowed for the comparison between the different images. A qualitative descriptive comparison was performed between the calcified drusen seen on CF images and their appearance on FAF, NIR, and *en face* SS OCT images.

Results

Two hundred twenty eyes from 139 patients with nonexudative AMD were identified. The median age of the patients was 78 years (age range, 56–97 years), and 65.5% were women (91/139). Of the 220 eyes, 94 eyes (42.7%) were found to have calcified drusen either at baseline or during the study period. In addition, 6 eyes were observed to show that some of the calcified drusen had regressed without cRORA developing during follow-up, which was confirmed on the respective CF, NIR, FAF, and *en face* SS OCT images. The cases of 5 representative patients are described, demonstrating our observations of how calcified drusen appear on multimodal imaging and their eventual progression to cRORA, with an emphasis on the appearance of these lesions on *en face* SS OCT imaging.

Patient 1

Images obtained from a 76-year-old man with a history of nonexudative AMD in the left eye are shown in Figures 1 and 2. Figure 1 shows the same-day *en face* multimodal images of the patient's left eye at 3 visits over a 2-year period. The CF images served as the reference for identifying calcified drusen and pigment deposits. At the baseline visit, the CF image shows drusen with corresponding RPE elevations on the drusen volume map (Fig 1 A, E, white arrows). One druse can be seen on the representative B-scan (Fig 2B, yellow arrow), and it eventually became calcified at the 1-year and 2-year follow-up visits (Fig 1F–O, yellow and blue arrows). In addition to the drusen, dark spots were observed that represent pigmentary deposits on the CF image (Fig 1A, green arrow). On the NIR image, these pigment deposits appear as bright foci or hyperreflective lesions (Fig 1B, green arrow). In contrast, the *en face* SS OCT image displays the pigment deposits as dark areas or hypoTDs (Fig 1D, green arrow). On the corresponding B-scan, the pigment deposits appear as hyperreflective foci in the retina (Fig 2C, white arrow). At the 1-year visit, the calcified druse presented as a bright yellow lesion with defined borders on the CF image (Fig 1F, yellow arrow). When compared with the CF images, the NIR and the *en face* SS OCT images seemed to detect the calcified druse and pigment deposits, whereas the FAF images did not show these lesions. On the NIR image, the calcified druse is shown as a hyperreflective lesion (Fig 1G, yellow arrow). On the *en face* SS OCT image, the calcified druse is present as a dark area or hypoTD (Fig 1I, yellow arrow), which is similar to the pigment deposits. However, on the corresponding B-scans, the calcified druse contains a hyperreflective cap with choroidal hypotransmission beneath the lesion (Fig 2F, yellow arrow), whereas the pigment deposits appear as hyperreflective foci in the retina (Fig 2G, H, white arrows). At the 2-year follow-up visit, the calcified druse was more prominent on the CF, NIR, and *en face* SS OCT images (Fig 1K, L, N, blue arrows). The corresponding B-scan shows the calcified druse with a heterogenous internal reflectivity along with the hyperreflective cap and choroidal hypotransmission beneath the druse (Fig 2J, K, yellow arrows), whereas the pigment deposits correspond to the hyperreflective foci in the retina (Fig 2K, L, white arrows). Thus, unlike the NIR images, the calcified druse and pigment deposits can be distinguished on the *en face* SS OCT images by looking at the corresponding B-scans.

Patient 2

Images obtained from a 73-year-old woman with a history of nonexudative AMD in the right eye are shown in Figures 3 and 4. Figure 3 shows the same-day *en face* multimodal images of the patient's right eye at 3 visits over a 4-year period. At the baseline visit, the CF image showed soft drusen that corresponded to the drusen volume map (Fig 3A, E, white arrows). In addition, the drusen can be appreciated on the corresponding B-scans (Fig 4C, D,

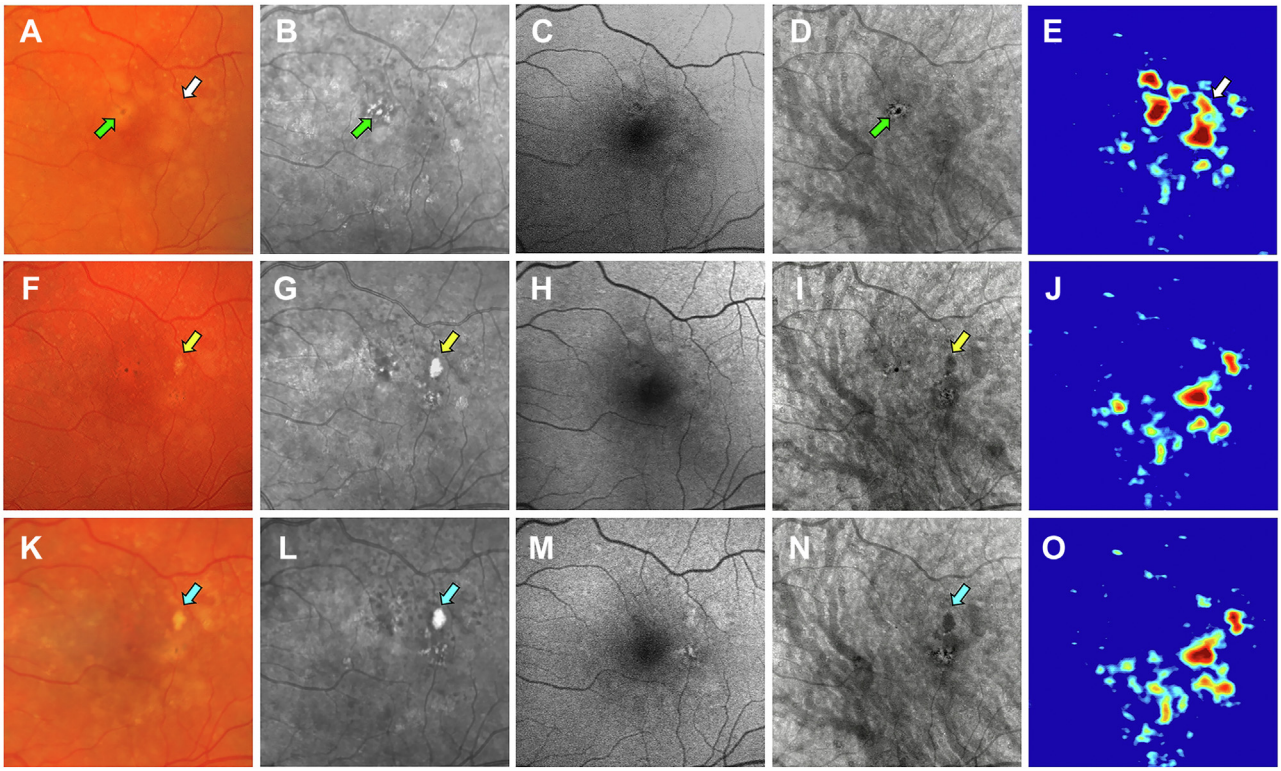

Figure 1. Multimodal imaging of the left eye of a 76-year-old man obtained over a 2-year period: (**A**–**E**) baseline visit, (**F**–**J**) 1-year follow-up visit, and (**K**–**O**) 2-year follow-up visit; (**A**, **F**, **K**) color fundus (CF) images, (**B**, **G**, **L**) near infrared (NIR) images, (**C**, **H**, **M**) fundus autofluorescence (FAF) images, (**D**, **I**, **N**) *en face* swept source (SS) OCT images, and (**E**, **J**, **O**) drusen volume maps. **A**–**E**, Images obtained at baseline showing a soft druse that is identified by the white arrow on the CF image (**A**) and corresponds to the druse on the volume map (**E**, white arrow). This druse ultimately became calcified, which is shown in the 1-year and 2-year follow-up visit images. In addition, visible pigment deposits are represented by dark spots in the CF image (**A**, green arrow). On the NIR image, the pigment deposits are shown as hyperreflective areas (**B**, green arrow). On the *en face* SS OCT image, the pigment deposits are represented as dark areas or hypotransmission defects (hypoTDs) (**D**, green arrow). **F**–**J**, Images obtained at the 1-year visit showing a calcified druse appearing as a bright yellow lesion with defined borders on the CF image (**F**, yellow arrow). The NIR image displays the calcified druse as a hyperreflective lesion (**G**, yellow arrow). The pigment deposits also appear as bright spots on the NIR image. The FAF image (**H**) fails to reliably identify the calcified druse and pigment deposits. On the *en face* SS OCT image, the calcified druse appears as a dark area or hypoTD (**I**, yellow arrow). Similarly, the pigment deposits are displayed as small hypoTDs. **K**–**O**, Images obtained at the 2-year visit showing further progression of the calcified druse, identified by the blue arrows on the CF (**K**), NIR (**L**), and *en face* SS OCT (**N**) images.

yellow and white arrows). These drusen ultimately became calcified with the appearance of pigment deposits, which first became visible at the 2-year follow-up visit (Fig 3F–J). On the CF image, the calcified drusen appear as bright yellow lesions with defined borders and glistening dots within the drusen (Fig 3F, yellow arrows), whereas the pigment deposits are displayed as dark spots. On the NIR images, the calcified drusen and pigment deposits are shown as bright or hyperreflective regions (Fig 3G, yellow arrows). On the *en face* SS OCT images, the calcified drusen and pigment deposits appear as hypoTDs (Fig 3I, yellow arrows). However, the corresponding B-scans can distinguish between hyperreflective pigment deposits in the retina (Fig 4H, white arrow) and the calcified drusen that have a heterogeneous internal reflectivity along with a hyperreflective cap (Fig 4G, yellow arrow). At the 4-year follow-up visit, the calcified drusen had enlarged with more lesions developing, as shown on the CF, NIR, and *en face* SS OCT images (Fig 3K, L, N, blue arrows). On the corresponding B-scans, the hypoTDs are mostly caused by calcified drusen with a hyperreflective cap and heterogenous internal reflectivity, whereas the pigment deposits have only a minor contribution (Fig 4K, L, yellow and white arrows). Thus, similar to the previous patient, both the pigment deposits and the calcified drusen are associated with the choroidal hypoTDs on the *en face* SS OCT image, but they can be differentiated by reviewing the corresponding B-scans.

Patient 3

Images obtained from a 74-year-old woman with a history of nonexudative AMD in the left eye are shown in Figures 5 and 6. Figure 5 shows the same-day *en face* multimodal images of the patient's left eye at 3 visits over a 2-year period. At the baseline visit, calcified drusen can be seen on the CF, NIR, *en face* SS OCT images and corresponding B-scans (Figs 5A, B, D and 6C, yellow arrows). At the 1-year follow-up visit, atrophy could be seen forming around the calcified drusen. This can be appreciated on the

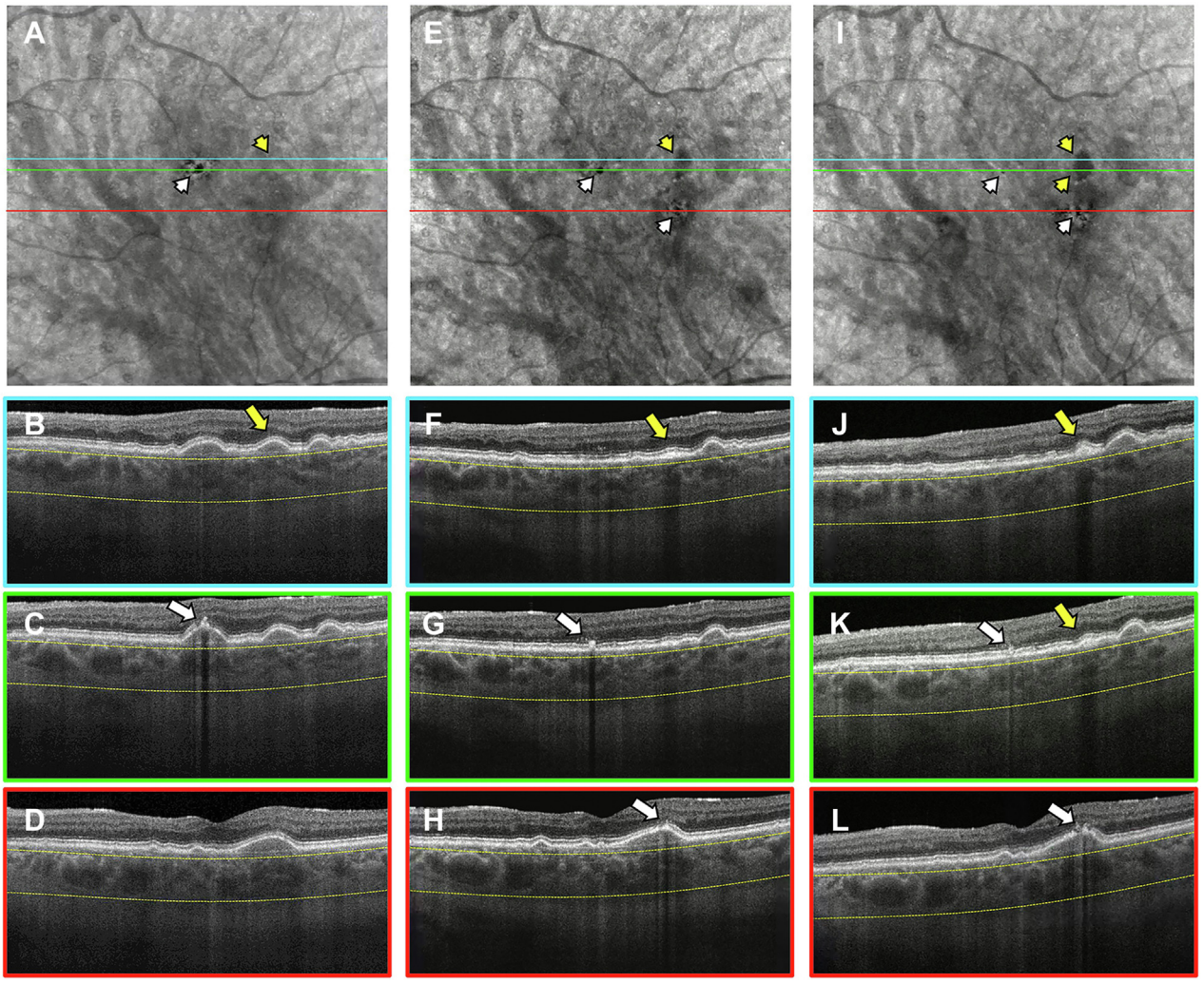

Figure 2. *En face* swept-source (SS) OCT images with color-coded B-scans from the left eye of a 76-year-old man obtained at the (**A**–**D**) baseline, (**E**–**H**) 1-year, and (**I**–**L**) 2-year visits. The *en face* SS OCT image was created using a slab positioned from 64 to 400 μm under Bruch's membrane. **A**–**D**, Images obtained at the baseline visit displaying a soft druse on the corresponding B-scan that later became calcified (**B**, yellow arrow) and is not identifiable on the *en face* image (**A**, yellow arrowhead). In addition, hyperreflective foci or pigment deposits can be seen at this visit (**C**, white arrow) and cause a hypotransmission defect (hypoTD) on the *en face* SS OCT image (**A**, white arrowhead). **E**–**H**, Images obtained at the 1-year visit showing a hypoTD on the *en face* SS OCT image (**E**, yellow arrowhead) caused by the calcified druse with a hyperreflective cap on the corresponding B-scan (**F**, yellow arrow). In addition, small hypoTDs on the *en face* SS OCT image (**E**, white arrowheads) are the result of pigment deposits and can be seen as hyperreflective foci in the retina on the corresponding B-scans (white arrows in (**G**) and (**H**)). **I**–**L**, Images obtained at the 2-year visit showing hypoTDs on the *en face* SS OCT image that correspond to the calcified druse (**I**, yellow arrowheads) and pigment deposits (**I**, white arrowheads). On the corresponding B-scans, the yellow arrows identify the calcified druse with a hyperreflective cap and heterogenous internal reflectivity (**J**, **K**), whereas the white arrows identify the pigment deposits as retinal hyperreflective foci (**K**, **L**).

FAF image that shows areas of hypoautofluorescence (Fig 5H, blue arrow) and on the *en face* SS OCT image that displays areas of choroidal hyperTDs at the same location (Fig 5I, blue arrow). These regions of choroidal hyperTDs can be seen on the corresponding B-scans, along with attenuation of the outer nuclear layer (Fig 6G, H, yellow and white arrows). At the 2-year follow-up visit, the FAF image displayed hypoautofluorescence in the region of the calcified drusen (Fig 5M, red arrow), indicating that the RPE overlying the calcified drusen and its surrounding area had progressed to atrophy. In contrast, the *en face* SS OCT image displays hyperTDs around a portion of the calcified drusen corresponding to cRORA and hypoTDs representing the remaining calcified drusen (Fig 5N, red arrow). The corresponding B-scans show both the choroidal hypertransmission around the calcified drusen and the choroidal hypotransmission beneath the lesion (Fig 6K, L, yellow and white arrows).

Patient 4

Images obtained from a 68-year-old woman with a history of nonexudative AMD in the left eye are shown in Figures 7 and 8. Figure 7 shows the same-day *en face* multimodal

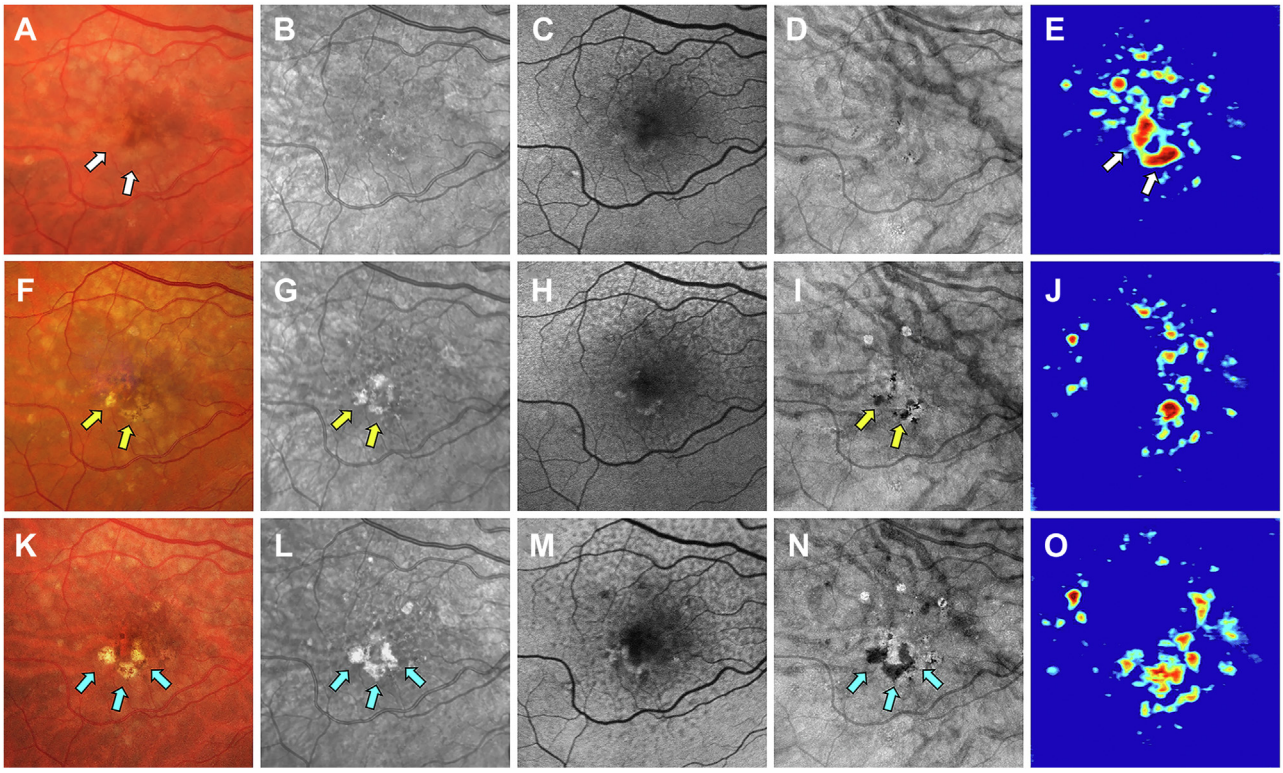

Figure 3. Multimodal imaging of the right eye of a 73-year-old woman obtained over a 4-year period: (**A**–**E**) baseline visit, (**F**–**J**) 2-year follow-up visit, and (**K**–**O**) 4-year follow-up visit; (**A**, **F**, **K**) color fundus (CF) images, (**B**, **G**, **L**) near infrared (NIR) images, (**C**, **H**, **M**) fundus autofluorescence (FAF) images, (**D**, **I**, **N**) *en face* swept-source (SS) OCT images, and (**E**, **J**, **O**) drusen volume maps. **A**–**E**, Images obtained at baseline showing soft drusen on the CF image (**A**, white arrows) that correspond to the drusen on the volume map (**E**, white arrows). These drusen ultimately became calcified, which was observed at the 2-year and 4-year follow-up visits. **F**–**J**, Images obtained at the 2-year visit showing calcified drusen appearing as bright yellow lesions with defined borders containing glistening dots (**F**, yellow arrows) along with pigment deposits on the CF image. The NIR image (**G**) shows calcified drusen and pigment deposits appearing as hyperreflective lesions (yellow arrows). The FAF image (**H**) fails to reliably identify the calcified drusen or pigment deposits. On the *en face* SS OCT image (**I**), the calcified drusen and pigment deposits appear as dark areas or hypotransmission defects (yellow arrows). **K**–**O**, Images obtained at the 4-year visit showing the formation of more calcified drusen as shown by the blue arrows on the CF (**K**), NIR (**L**), and *en face* SS OCT (**N**) images.

images of the patient's left eye at 3 visits over a 2-year period. At the baseline visit, several calcified drusen could be seen on the CF, NIR, *en face* SS OCT images and corresponding B-scans (Figs 7A, B, D and 8B–E, yellow arrows). At the 1-year follow-up visit, a hyperTD could be seen around the periphery of one of the hypoTDs on the *en face* OCT image (Fig 7I, blue arrow). This is referred to as a *donut lesion* and is defined as hyperTDs surrounding a hypoTD core. As mentioned in the case of patient 3, the *en face* SS OCT image can detect hyperTDs around the borders of the calcified drusen as cRORA develops, with the remaining calcified material creating the hypoTD. In contrast, the FAF image for this visit barely shows a detectable hypoautofluorescent lesion at the location of the calcified drusen because of the overlying retinal luteal pigments (Fig 7H, blue arrow). The corresponding B-scan displays choroidal hypertransmission around the calcified drusen with choroidal hypotransmission beneath the lesion (Fig 8J, white arrow). At the 2-year follow-up visit, additional donut lesions were present on the *en face* SS OCT image (Fig 7N, red arrows), and these donut lesions correspond to the regions of hypoautofluorescence seen on the FAF image (Fig 7M, red arrows). Thus, atrophy of calcified drusen creates the donut lesions that are seen on the *en face* OCT images and correlate with the regions of hypoautofluorescence on the FAF images. Corresponding B-scans for this visit confirm the presence of choroidal hypertransmission around the calcified drusen with choroidal hypotransmission beneath the lesions (Fig 8L, M, O, blue arrows).

Patient 5

Images obtained from an 82-year-old woman with a history of nonexudative AMD in the left eye are shown in Figures 9 and 10. Figure 9 shows the same-day *en face* multimodal images of the patient's left eye at 3 visits over a 3-year period. At the baseline visit, 4 calcified drusen were identified on the CF, NIR, *en face* SS OCT images and corresponding B-scans (Figs 9A, B, D and 10B, C, yellow arrows). At the 1-year follow-up visit, these calcified drusen became more prominent and are identified by the blue arrows on the CF, NIR, and *en face* SS OCT images (Fig 9F, G, I). In addition, the corresponding B-scans display these

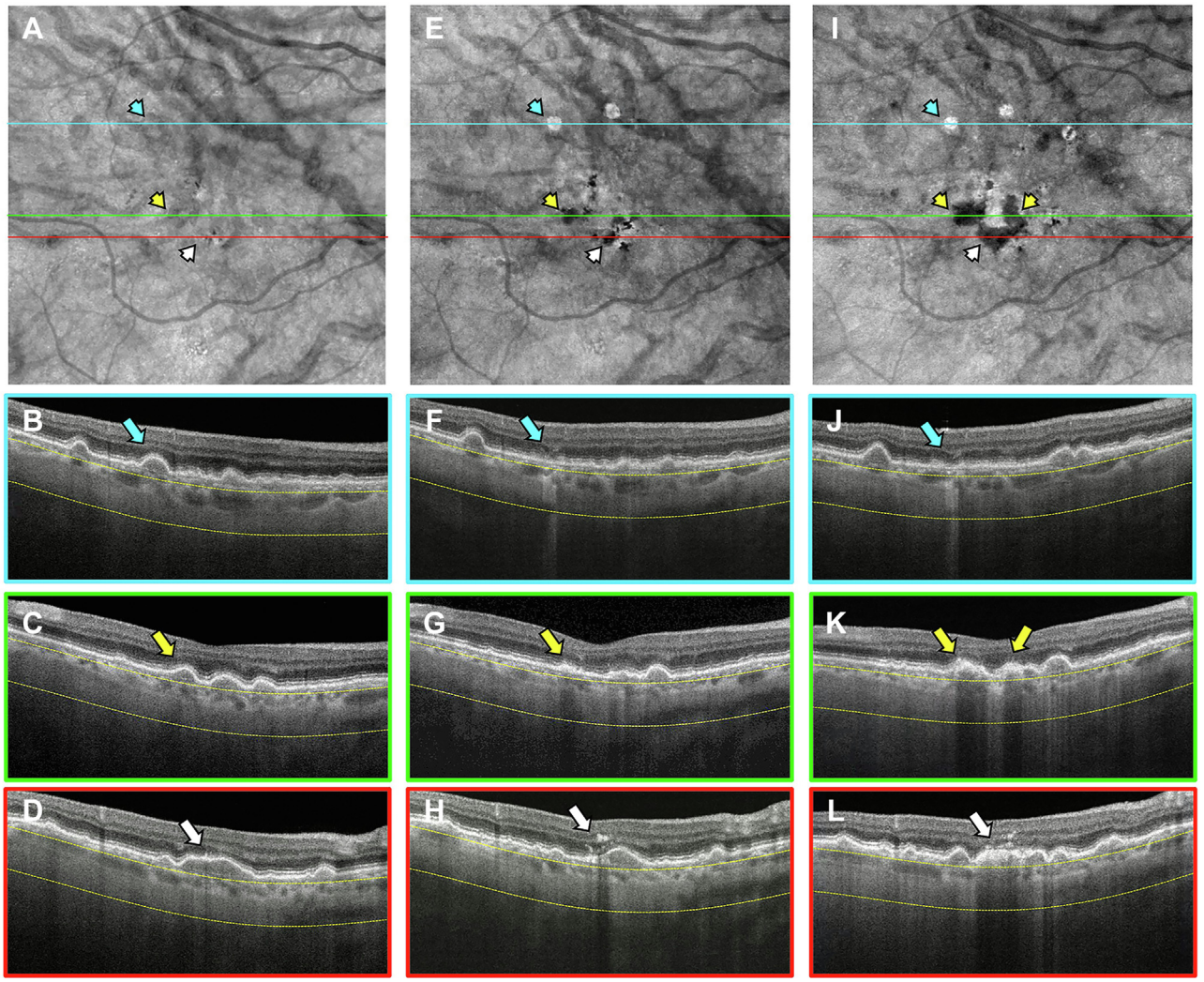

Figure 4. *En face* swept-source (SS) OCT images with color-coded B-scans of the right eye of a 73-year-old woman obtained at the (**A**–**D**) baseline, (**E**–**H**) 2-year, and (**I**–**L**) 4-year visits. The *en face* SS OCT image was created using a slab positioned from 64 to 400 μm under Bruch's membrane. **A**–**D**, Images obtained at the baseline visit showing soft drusen on the corresponding B-scans (yellow and white arrows in [**C** and **D**]) that are not identifiable on the *en face* SS OCT image (**A**, yellow and white arrowheads). These drusen later became calcified. **E**–**H**, Images obtained at the 2-year visit showing that hypotransmission defects (hypoTDs) on the *en face* SS OCT image (**E**, yellow and white arrowheads) are caused by a calcified drusen with a hyperreflective cap (**G,** yellow arrow) and hyperreflective foci or pigment deposits in the retina (**H**, white arrow). **I**–**L**, Images obtained at the 4-year visit showing hypoTDs on the *en face* SS OCT image (**I**, yellow and white arrowheads) that correspond to the calcified drusen with a hyperreflective cap and heterogeneous internal reflectivity (yellow and white arrows in [**K**] and [**L**]) with a minor contribution from the retinal hyperreflective foci. For the B-scans color-coded in blue (**B**, **F**, **J**), the baseline visit displays a soft drusen on the corresponding B-scan (**B**, blue arrow) that is not identifiable on the *en face* SS OCT image (**A**, blue arrowhead). At the 2-year and 4-year visits, this soft drusen progressed to atrophy without appearing to develop calcific properties and displayed a hypertransmission defect on the *en face* SS OCT images (blue arrowheads in (**E**) and (**I**)). Consequently, choroidal hypertransmission and attenuation of the outer nuclear layer appear in the corresponding B-scans (blue arrows in [**F**] and [**J**]).

calcified drusen with a hyperreflective cap and choroidal hypotransmission beneath the lesions (Fig 10G, H, yellow arrows). At the 3-year follow-up visit, these calcified drusen had regressed without atrophy developing. This is demonstrated by the FAF image showing no hypoautofluorescence (Figs 9M, green arrows) and the *en face* SS OCT image displaying no hyperTDs in the areas where the calcified drusen existed (Figs 9N, green arrows). However, on the corresponding B-scans, deposits along the RPE were present in the same area where the calcified drusen previously resided (Fig 10L, M, white arrows). Also, attenuation of the outer nuclear layer was present in the same region of the regressed calcified drusen. In addition, the CF and NIR images confirmed the regression of these lesions (Fig 9K, L, green arrows). This patient also harbored areas of hyperTDs on the *en face* SS OCT image and corresponding B-scans that seemed to develop from drusen without calcific properties and were detected at the time of the follow-up visits (Figs 9N, red arrows; Fig 10M–O, blue arrows). Thus, this patient demonstrated

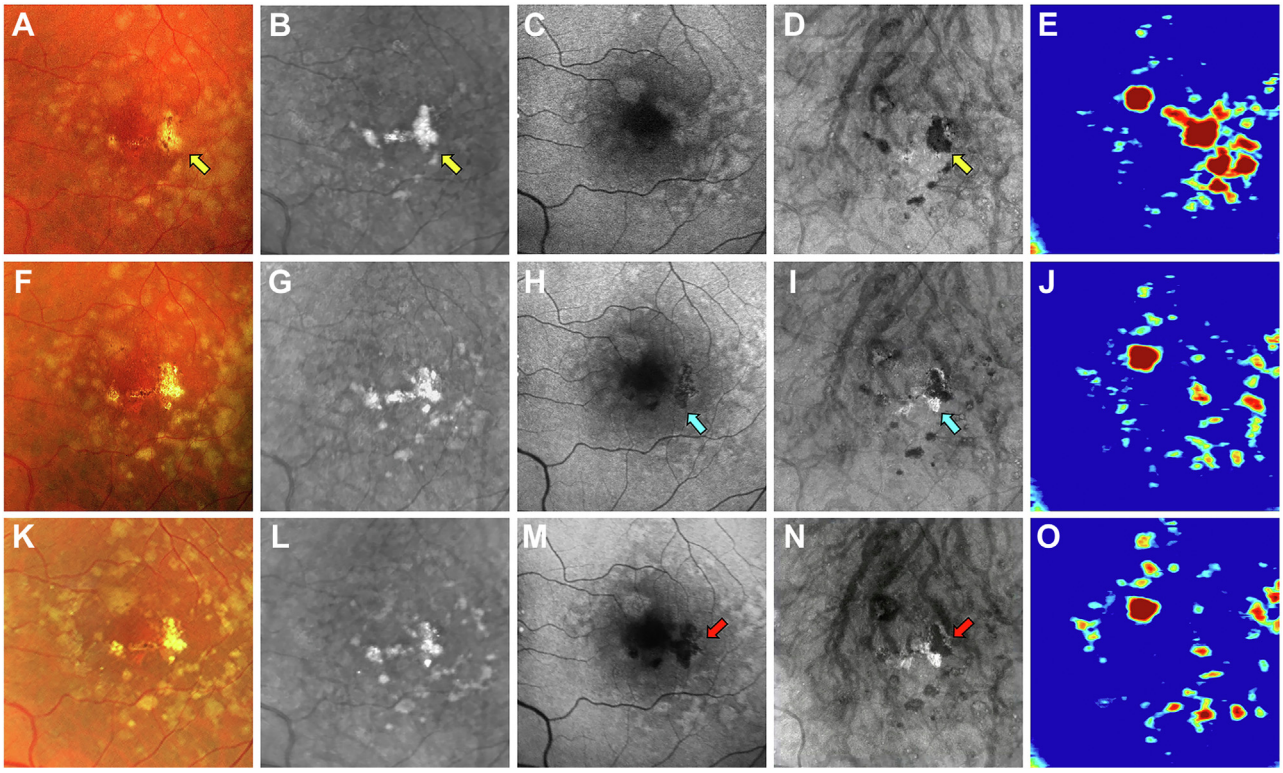

Figure 5. Multimodal imaging of the left eye of a 74-year-old woman obtained over a 2-year period: (**A**–**E**) baseline visit, (**F**–**J**) 1-year follow-up visit, and (**K**–**O**) 2-year follow-up visit; (**A**, **F**, **K**) color fundus (CF) images, (**B**, **G**, **L**) near infrared (NIR) images, (**C**, **H**, **M**) fundus autofluorescence (FAF) images, (**D**, **I**, **N**) *en face* swept-source (SS) OCT images, and (**E**, **J**, **O**) drusen volume maps. **A**–**E**, Images obtained at baseline showing a calcified drusen on the CF image (**A**) as a bright yellow lesion with defined borders (yellow arrow). In addition, the NIR image (**B**) displays the calcified drusen as a hyperreflective region (yellow arrow). The *en face* SS OCT image (**D**) shows this calcified drusen as a hypotransmission defect (hypoTD; yellow arrow). **F**–**J**, Images obtained at the 1-year visit showing atrophy forming around the calcified drusen. This is displayed through the FAF image (**H**) showing patches of hypoautofluorescence (blue arrow). In addition, the *en face* SS OCT image (**I**) shows hypertransmission defects (hyperTDs) in the same region (blue arrow). **K**–**O**, Images obtained at the 2-year visit, with the FAF image (**M**) showing hypoautofluorescence in the entire area of the calcified drusen (red arrow), which indicates that the retinal pigment epithelium both above and around the calcified drusen has progressed to atrophy. In contrast, the *en face* SS OCT image (**N**) displays only hyperTDs around the lesion (red arrow) because the calcified drusen causes a hypoTD.

that an eye can contain different types of precursor lesions with some progressing to cRORA and others spontaneously regressing without visible sequelae during the follow-up period.

Discussion

Calcified drusen have been described as bright yellow lesions with defined borders containing glistening dots on CF images.[7–10] On OCT B-scan imaging, these lesions have been shown to correspond to drusen with heterogeneous internal reflectivity or hyporeflective internal cores along with a hyperreflective cap.[5–9,30–32] In addition, these drusen were reported to contain crystalline calcium phosphate deposits that were called *calcific nodules* on histopathologic examination.[7,8] In this study, we used multimodal imaging to observe the development and progression of calcified drusen and showed that *en face* OCT imaging is a convenient method for the detection and monitoring of these lesions, with most of them progressing to cRORA. From our analysis, 42.7% of eyes with nonexudative AMD were found to have calcified drusen either at baseline or during follow-up. Thus, calcified drusen are common in eyes with AMD and should be considered a highly predictive precursor lesion for the development of cRORA, which is consistent with the work of previous studies investigating calcified drusen.[5–12]

On NIR imaging, calcified drusen appear as bright hyperreflective lesions that correspond to the hypoTDs seen on *en face* SS OCT imaging. However, when using NIR imaging alone, it is impossible to distinguish between calcified drusen and pigment deposits. In addition, FAF imaging proved unreliable for the purpose of identifying calcified drusen until they developed into hypoautofluorescent foci consistent with cRORA. Furthermore, the presence of macular xanthophylls can obscure the detection of atrophic calcified drusen located in the foveal region on FAF images. Although OCT B-scans can reliably detect calcified drusen as having heterogeneous internal reflectivity, hyporeflective cores, and hyperreflective caps, it is a laborious process to meticulously review every B-scan in an entire OCT raster scan. In contrast, *en face* OCT

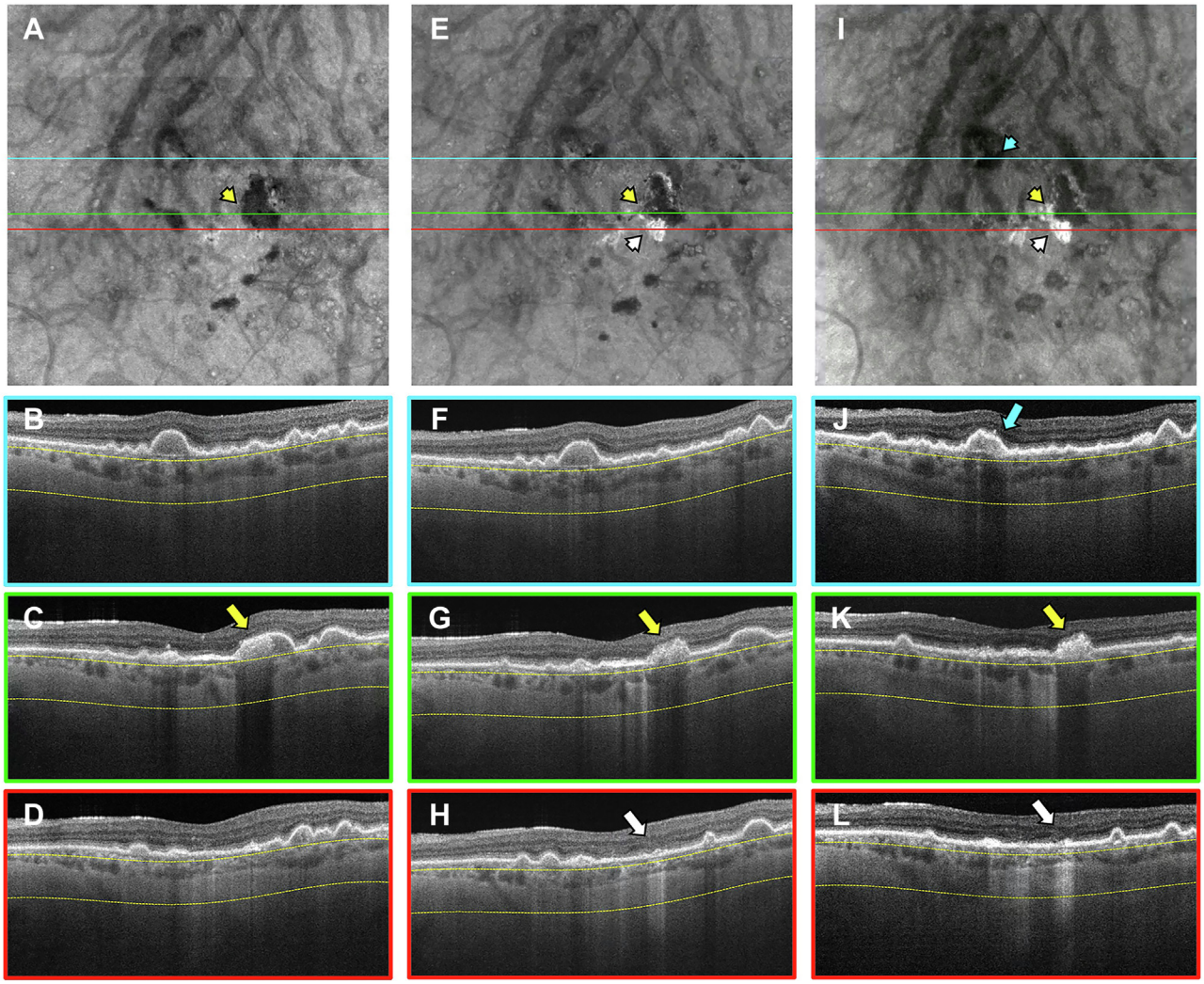

Figure 6. *En face* swept-source (SS) OCT images with color-coded B-scans of the left eye of a 74-year-old woman obtained at (**A**–**D**) baseline, (**E**–**H**) 1-year follow-up visit, and (**I**–**L**) 2-year follow-up visit. The *en face* SS OCT image was created using a slab positioned from 64 to 400 μm beneath Bruch's membrane. **A**–**D**, Images obtained at the baseline visit displaying calcified drusen, which are represented as a hypotransmission defect (hypoTD) on the *en face* SS OCT image (**A**, yellow arrowhead). The corresponding B-scan (**C**) shows a calcified drusen with a heterogenous internal reflectivity and choroidal hypotransmission beneath a portion of the drusen (yellow arrow). **E**–**H**, Images obtained at the 1-year visit showing hypertransmission defects (hyperTDs) that can be observed around the calcified drusen on the *en face* SS OCT image (**E**, yellow and white arrowheads). The corresponding B-scans (**G**, **H**) show choroidal hypertransmission and attenuation of the outer nuclear layer (ONL) next to the calcified drusen (yellow and white arrows). Because of the calcified material within the drusen creating a hypoTD, the *en face* SS OCT image can display only hyperTDs around the calcified drusen. **I**–**L**, Images obtained at the 2-year visit showing that the hyperTD has increased around the periphery of the hypoTD on the *en face* SS OCT image (**I**, yellow and white arrowheads). Similarly, the corresponding B-scans (**K**, **L**) display choroidal hypertransmission next to the calcified drusen and attenuation of the ONL both on top and around the calcified drusen (yellow and white arrows). In addition, the color-coded B-scan in blue (**J**) displays a newly formed calcified drusen with heterogenous internal reflectivity and choroidal hypotransmission beneath the lesion (blue arrow) and corresponds to the hypoTD on the *en face* SS OCT image (**I**, blue arrowhead).

imaging is a simpler method for the detection of calcified drusen because it allows the reviewer to screen the entire volumetric scan with a single glance. As soon as the hypoTDs are identified on the *en face* image, the corresponding B-scans can be reviewed to confirm the presence of calcified drusen. As a result, *en face* OCT imaging with the aid of corresponding B-scans can be used as a stand-alone method for detecting and monitoring calcified drusen.

The ability of *en face* OCT imaging to identify calcified drusen relies on the detection of hypoTDs that are created by these lesions on a sub-RPE slab. The hypoTD produced by the calcified drusen most likely results from the calcific nodules within the drusen that attenuate or scatter the incident and reflected light before reaching the detector of the OCT instrument. This property of calcified drusen was first described by Suzuki et al,[7] who proposed that the calcium nodules in the drusen create multiple

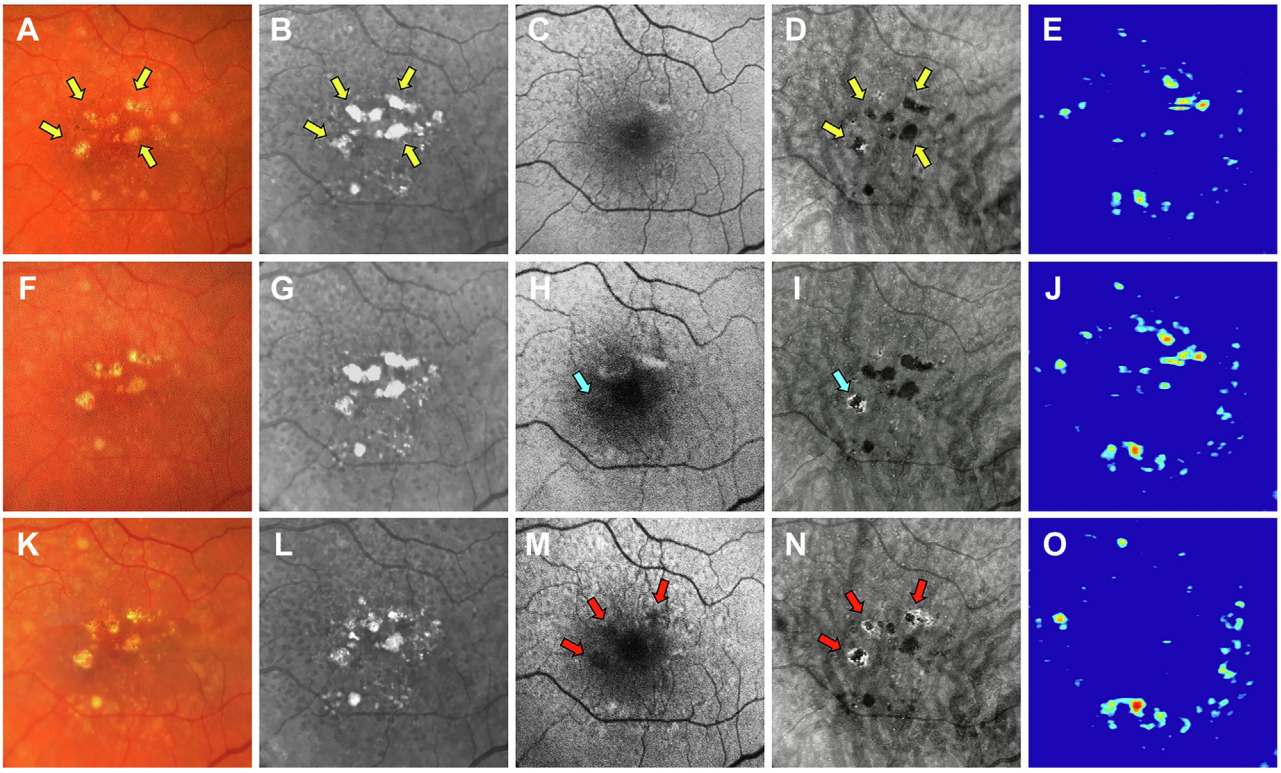

Figure 7. Multimodal imaging of the left eye of a 68-year-old woman obtained over a 2-year period: (**A**–**E**) baseline visit, (**F**–**J**) 1-year follow-up visit, and (**K**–**O**) 2-year follow-up visit; (**A**, **F**, **K**) color fundus (CF) images, (**B**, **G**, **L**) near infrared (NIR) images, (**C**, **H**, **M**) fundus autofluorescence (FAF) images, (**D**, **I**, **N**) *en face* swept-source (SS) OCT images, and (**E**, **J**, **O**) drusen volume maps. **A**–**E**, Images obtained at the baseline visit displaying several calcified drusen on the CF (**A**), NIR (**B**), and *en face* SS OCT (**D**) images that are depicted by the yellow arrows. **F**–**J**, Images obtained at the 1-year visit displaying a hypertransmission defect (hyperTD) around the periphery of one of the hypotransmission defects (hypoTD) on the *en face* SS OCT image (**I**, blue arrow). This is known as a donut lesion, which is defined as hyperTDs surrounding a hypoTD core. This is the result of the *en face* SS OCT image being able to detect hyperTDs around the borders of the calcified drusen, but not above the lesion, because the calcified material within the drusen attenuates or scatters the incident light from the SS OCT instrument. In contrast, the FAF image (**H**) displays hypoautofluorescence in the entire area of the calcified drusen (blue arrow), which demonstrates that atrophy develops both on top and around the area of the calcified drusen. As a result, donut lesions on the *en face* SS OCT image represents calcified drusen that has progressed to atrophy. **K**–**O**, Images obtained at the 2-year visit showing more donut lesions that developed on the *en face* SS OCT image (**N**) that are depicted by the red arrows. In addition, the FAF image (**M**) displays hypoautofluorescence in the same area as the donut lesions (red arrows).

reflecting surfaces that attenuate the light before it returns to the detector. This proposal was confirmed by the corresponding B-scans that showed choroidal hypotransmission beneath the calcified drusen; these features were also seen in the study by Suzuki et al.[7]

In addition to *en face* OCT imaging identifying calcified drusen as hypoTDs, this method has the added advantage of detecting the formation of RPE atrophy within and around the area of the calcified drusen by the appearance of hyperTDs. As previously reported, hyperTDs with a greatest linear dimension of $\geq$250 μm have been shown to correspond to the formation of cRORA.[25–27] We observed that atrophy first becomes detectable around the periphery of the hypoTD, creating the appearance of a donut lesion, and correlates with atrophy of the RPE overlying the calcified drusen. As a result, cRORA eventually develops in the area outlined by both the hyperTDs and hypoTDs on the *en face* OCT image. This was confirmed by inspecting the corresponding FAF images that showed hypoautofluorescence in the same area of the calcified drusen, although the *en face* OCT images only displayed hyperTDs around the hypoTDs (Figs 5 and 7). In fact, the donut lesions correlate well with the images shown by Suzuki et al,[7] who found a generalized loss of autofluorescence signal over the calcified drusen, which appeared to spread across a larger area than each druse. Because these observations verify our clinical experience that these donut lesions progress to cRORA, we propose to include the entire area of the donut, which encompasses both the hyperTDs and hypoTDs, as a region that will irreversibly evolve into conventional cRORA. As a result, we suggest that these donut lesions should be considered equivalent to cRORA when defining disease progression. Natural history studies using *en face* OCT imaging in eyes with AMD are currently underway to test this proposal.

From our patients, we observed that calcified drusen originate from soft drusen, with most of them progressing to cRORA. We did observe in 6 patients that the calcified

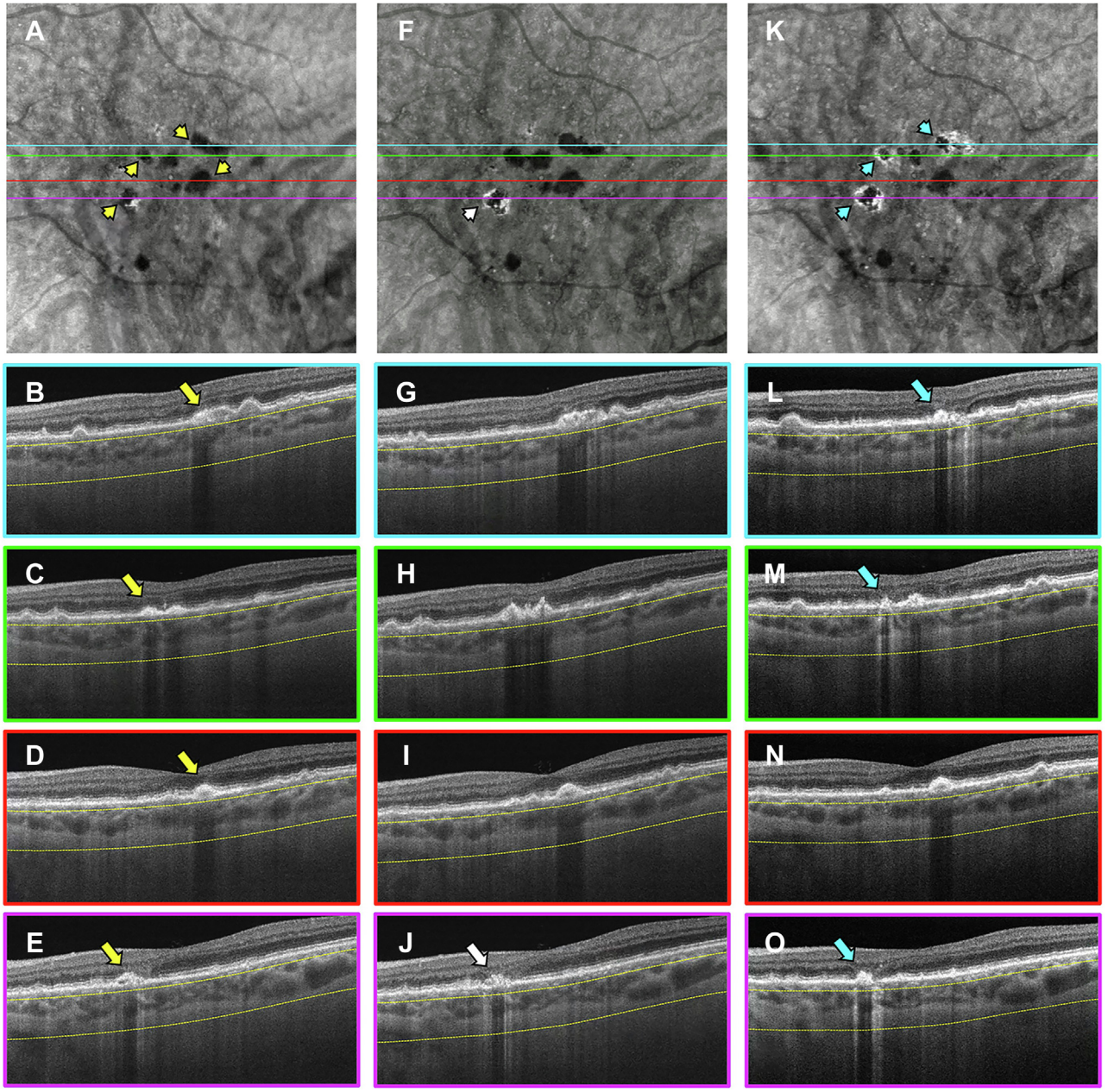

Figure 8. *En face* swept-source (SS) OCT images with color-coded B-scans of the left eye of a 68-year-old woman obtained at (**A**–**E**) baseline, (**F**–**J**) 1-year follow-up visit, and (**K**–**O**) 2-year follow-up visit. The *en face* SS OCT image was created using a slab positioned from 64 to 400 μm beneath Bruch's membrane. **A**–**E**, Images obtained at the baseline visit showing several calcified drusen represented as hypotransmission defects (hypoTDs) on the *en face* SS OCT image (**A**, yellow arrowheads). In addition, the corresponding B-scans (**B**–**E**) display these calcified drusen as having a heterogenous internal reflectivity with a hyperreflective cap and choroidal hypotransmission beneath the lesions (yellow arrows). **F**–**J**, Images obtained at the 1-year visit showing that one of the hypoTDs on the *en face* SS OCT image has a hypertransmission defect (hyperTD) surrounding it (**F**, white arrowhead). This is known as a donut lesion and is a sign that the entire area of the calcified drusen has progressed to atrophy. Consequently, the corresponding B-scan (**J**) shows choroidal hypertransmission around the calcified drusen and choroidal hypotransmission beneath the lesion (white arrow). In addition, attenuation of the outer nuclear layer encompassing the whole area of the calcified drusen is visible. **K**–**O**, Images obtained at the 2-year visit showing more donut lesions appearing on the *en face* SS OCT image (**K**, blue arrowheads) that are identified by the blue arrows in the corresponding B-scans (**L**, **M**, **O**).

drusen regressed without the formation of atrophy, which has been reported in a previous study.[10] However, B-scans through the respective areas showed deposits along the RPE with attenuation of the outer nuclear layer, where the calcified drusen previously existed (Fig 10). These deposits most likely represent remnants of the calcified drusen. As a result, the long-term implications of these regressed calcified drusen are being investigated in our

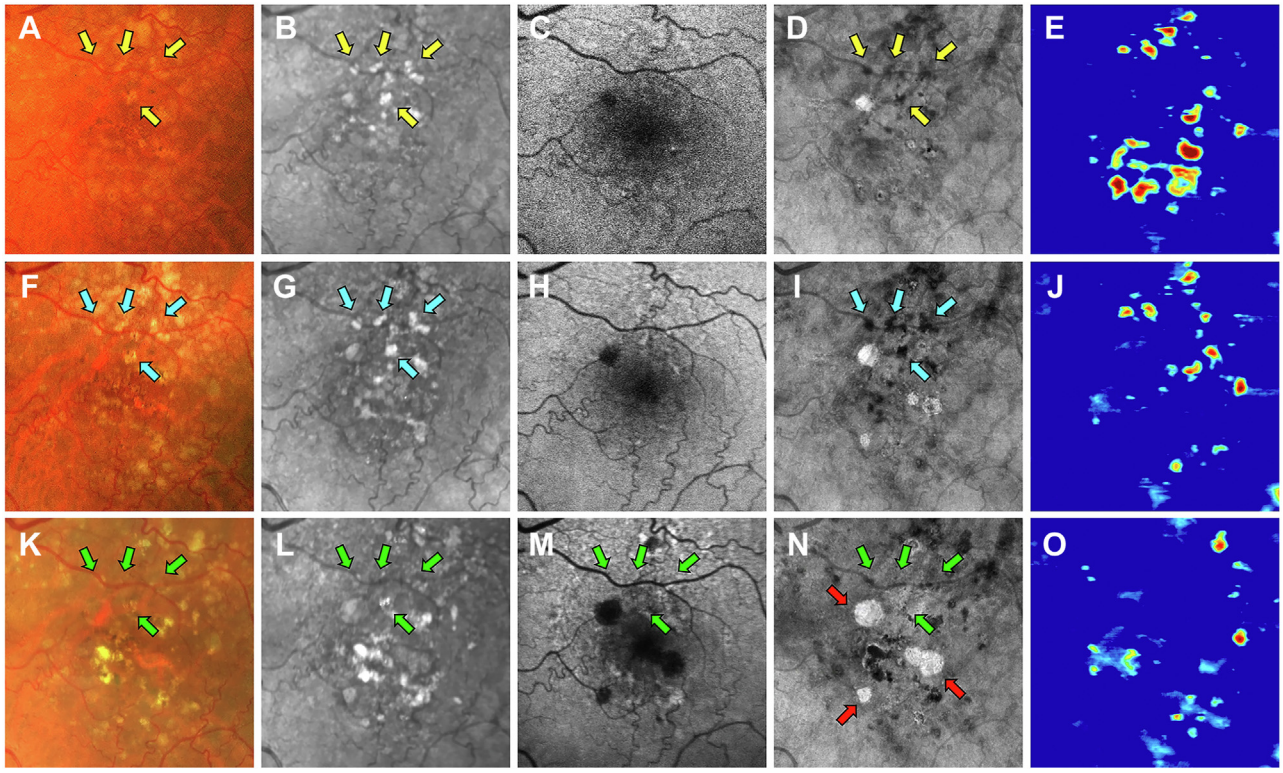

Figure 9. Multimodal imaging of the left eye of an 82-year-old woman obtained over a 3-year period (**A**–**E**) baseline visit, (**F**–**J**) 1-year follow-up visit, and (**K**–**O**) 3-year follow-up visit; (**A**, **F**, **K**) color fundus (CF) images, (**B**, **G**, **L**) near infrared (NIR) images, (**C**, **H**, **M**) fundus autofluorescence (FAF) images, (**D**, **I**, **N**) *en face* swept-source (SS) OCT images, and (**E**, **J**, **O**) drusen volume maps. **A**–**E**, Images obtained at baseline displaying several calcified drusen that are identified by the yellow arrows on the CF (**A**), NIR (**B**), and *en face* SS OCT (**D**) images. **F**–**J**, Images obtained at the 1-year visit showing that these calcified drusen remain and are identified by the blue arrows in the CF (**F**), NIR (**G**), and *en face* SS OCT (**I**) images. **K**–**O**, Images obtained at the 3-year visit showing that these calcified drusen regressed without atrophy developing. This is demonstrated through the FAF image (**M**) displaying no hypoautofluorescence (green arrows) and the *en face* SS OCT image (**N**) showing no hypertransmission defects (hyperTDs) in the region that the calcified drusen existed (green arrows). Moreover, the CF (**K**) and NIR (**L**) images confirm the regression of these lesions (green arrows). In addition, this case demonstrates that hyperTDs can form in the presence of drusen that do not appear to develop calcific features as identified by the red arrows on the *en face* SS OCT image (**N**).

ongoing natural history study. Interestingly, some eyes that contained regressed calcified drusen also harbored lesions that progressed to atrophy on *en face* OCT imaging. Although explanations for why some drusen become calcified and develop into cRORA remain elusive, it is intriguing to speculate that this type of disease progression may be associated with impairments of the underlying choriocapillaris, as suggested by other studies.[33–37]

Limitations of this study include its relatively small sample size and observational nature; however, the conclusions from the patients reported herein seem to be consistent with our observations from an ongoing natural history study. Although preliminary, the current report is designed to introduce the concept that the detection of hypoTDs on *en face* OCT images provides a practical and convenient method for identifying and studying the progression of calcified drusen. This is similar to the use of hyperTDs for detecting cRORA, which we demonstrated in previous publications.[25–27] As a result, ongoing studies looking at the natural history and progression of these lesions to cRORA will use our novel imaging strategy along with the more conventional multimodal imaging methods. In addition, these observations should prove useful in developing an automated algorithm that can identify and quantify calcified drusen for use in clinical practice and studies designed to assess the risk of disease progression in eyes with AMD.

In summary, this study used multimodal imaging to identify and characterize the evolution of calcified drusen in eyes with nonexudative AMD. Our results support previous findings showing that these prevalent lesions are an important risk factor for the progression of cRORA. We also demonstrated that *en face* OCT imaging can detect calcified drusen through the presence of choroidal hypoTDs, which can progress to donut lesions and cRORA. Although it is possible that small calcified drusen may resolve spontaneously, most calcified drusen seem to develop into atrophy. Thus, it remains to be determined if these lesions represent a risk factor for disease progression or a forme fruste of cRORA that should be excluded from studies that test therapies designed to prevent the progression to cRORA. Regardless of whether calcified drusen

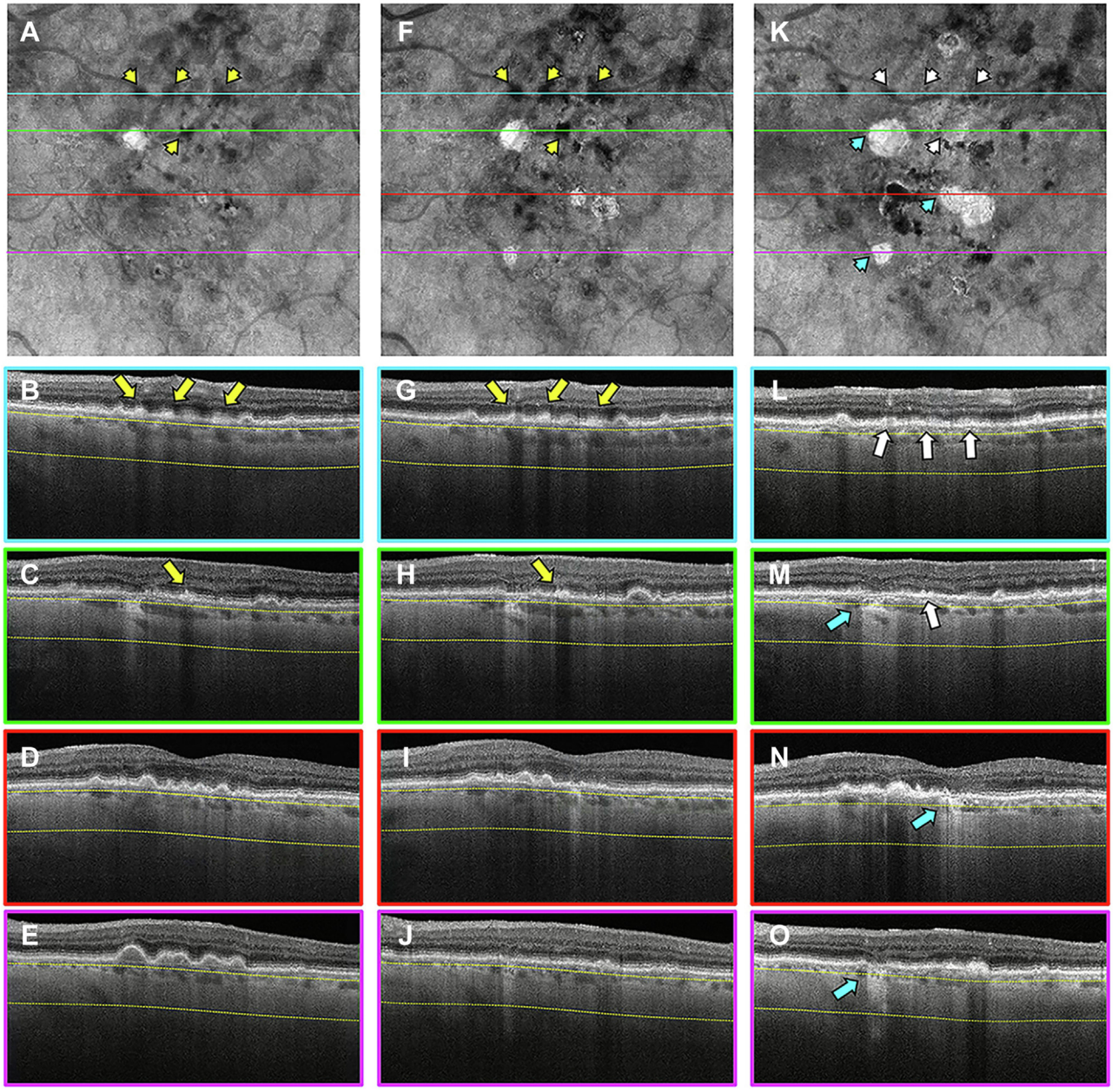

Figure 10. *En face* swept-source (SS) OCT images with color-coded B-scans of the left eye of an 82-year-old woman obtained at (**A**–**E**) baseline, (**F**–**J**) 1-year follow-up visit, and (**K**–**O**) 3-year follow-up visit. The *en face* SS OCT image was created using a slab positioned from 64 to 400 μm beneath Bruch's membrane. **A**–**E**, Images obtained at baseline displaying several calcified drusen as hypotransmission defects on the *en face* SS OCT image (**A**, yellow arrowheads). The corresponding B-scans (**B**, **C**) display these drusen with a hyperreflective cap and choroidal hypotransmission beneath the lesions (yellow arrows). **F**–**J**, Images obtained at the 1-year visit showing that these calcified drusen remain, as observed on the en face SS OCT image (**F**, yellow arrowheads), and are identified by the yellow arrows in the corresponding B-scans (**G**, **H**). **K**–**O**, Images obtained at the 3-year visit showing that the calcified drusen regressed without the formation of atrophy or hypertransmission defects (hyperTDs) on the *en face* SS OCT image (**K**, white arrowheads). However, on the corresponding B-scans (**L**, **M**), deposits along the retinal pigment epithelium appear in the same area where the calcified drusen existed (white arrows) as well as attenuation of the outer nuclear layer in those regions. In addition, the *en face* SS OCT image displays areas of hyperTDs that did not appear to develop from calcified drusen (**K**, blue arrowheads) and are identified by the blue arrows in the corresponding B-scans (**M**–**O**).

have reached the point of no return in the progression from drusen to cRORA, we propose that the use of *en face* OCT imaging to identify and monitor calcified drusen will be a valuable strategy for assessing the overall risk of disease progression and for managing expectations of patients with AMD.

Footnotes and Disclosures

Originally received: April 2, 2022.
Accepted: April 13, 2022.
Available online: April 20, 2022. Manuscript no. XOPS-D-22-00066

[1] Department of Ophthalmology, Bascom Palmer Eye Institute, University of Miami Miller School of Medicine, Miami, Florida.

[2] New England Eye Center, Tufts Medical Center, Boston, Massachusetts.

Disclosure(s):

All authors have completed and submitted the ICMJE disclosures form.

The author(s) have made the following disclosure(s): N.K.W.: Officeholder — Gyroscope Therapeutics; Financial support — Carl Zeiss Meditec, Nidek, Heidelberg Engineering; Lecturer — Nidek; Equity interest — Ocudyne

G.G.: Financial support — Carl Zeiss Meditec, Inc.; Patent (with the University of Miami) — Carl Zeiss Meditec, Inc.

P.J.R.: Consultant — Apellis, Boehringer-Ingelheim, Carl Zeiss Meditec, Chengdu Kanghong Biotech, InflammX/Ocunexus Therapeutics, Ocudyne, Regeneron Pharmaceuticals, Unity Biotechnology; Financial support — Carl Zeiss Meditec, Inc., Gyroscope Therapeutics, Stealth BioTherapeutics; Equity interest — Apellis, Valitor, Verana Health, Ocudyne

Supported by Carl Zeiss Meditec, Inc., Dublin, California; the Salah Foundation; the National Eye Institute, National Institutes of Health, Bethesda, Maryland (grant no.: P30EY014801); and Research to Prevent Blindness, Inc., New York, New York (unrestricted grant to the Department of Ophthalmology, University of Miami Miller School of Medicine). The funding organization had no role in the design or conduct of this research.

HUMAN SUBJECTS: Human subjects were included in this study. The institutional review board of the University of Miami Miller School of Medicine approved the study, and all patients signed an informed consent. The study was performed in accordance with the tenets of the Declaration of Helsinki and complied with the Health Insurance Portability and Accountability Act of 1996.

No animal subjects were included in this study.

Author Contributions:

Conception and design: Liu, Laiginhas, Rosenfeld

Analysis and interpretation: Liu, Laiginhas, Shen, Shi, Li, Trivizki, Waheed, Gregori, Rosenfeld

Data collection: Liu, Laiginhas, Rosenfeld

Obtained funding: N/A; study was performed as part of regular employment duties at the Bascom Palmer Eye Institute. No additional funding was provided.

Overall responsibility: Liu, Laiginhas, Shen, Shi, Li, Trivizki, Waheed, Gregori, Rosenfeld

Abbreviations and Acronyms:
AMD = age-related macular degeneration; **CF** = color fundus; **cRORA** = complete retinal pigment epithelium and outer retinal atrophy; **FAF** = fundus autofluorescence; **GA** = geographic atrophy; **hyperTD** = hypertransmission defect; **hypoTD** = hypotransmission defect; **NIR** = near-infrared; **RPE** = retinal pigment epithelium; **SS** = swept-source.

Keywords:
Age-related macular degeneration, Calcified drusen, *En face* OCT, Geographic atrophy.

Correspondence:
Philip J. Rosenfeld, MD, PhD, Bascom Palmer Eye Institute, 900 NW 17th Street, Miami, FL 33136. E-mail: prosenfeld@miami.edu.

References

1. Sarks JP, Sarks SH, Killingsworth MC. Evolution of soft drusen in age-related macular degeneration. *Eye (Lond)*. 1994;8(Pt 3):269–283.
2. Curcio CA. Soft drusen in age-related macular degeneration: biology and targeting via the oil spill strategies. *Invest Ophthalmol Vis Sci*. 2018;59(4):AMD160–AMD181.
3. Gregori G, Wang F, Rosenfeld PJ, et al. Spectral domain optical coherence tomography imaging of drusen in nonexudative age-related macular degeneration. *Ophthalmology*. 2011;118(7):1373–1379.
4. Cukras C, Agrón E, Klein ML, et al. Natural history of drusenoid pigment epithelial detachment in age-related macular degeneration: Age-Related Eye Disease Study report no. 28. *Ophthalmology*. 2010;117(3):489–499.
5. Ouyang Y, Heussen FM, Hariri A, et al. Optical coherence tomography-based observation of the natural history of drusenoid lesion in eyes with dry age-related macular degeneration. *Ophthalmology*. 2013;120(12):2656–2665.
6. Bonnet C, Querques G, Zerbib J, et al. Hyperreflective pyramidal structures on optical coherence tomography in geographic atrophy areas. *Retina*. 2014;34(8):1524–1530.
7. Suzuki M, Curcio CA, Mullins RF, Spaide RF. Refractile drusen: clinical imaging and candidate histology. *Retina*. 2015;35(5):859–865.
8. Tan ACS, Pilgrim MG, Fearn S, et al. Calcified nodules in retinal drusen are associated with disease progression in age-related macular degeneration. *Sci Transl Med*. 2018;10(466): eaat4544. https://doi.org/10.1126/scitranslmed.aat4544.
9. Veerappan M, El-Hage-Sleiman AM, Tai V, et al. Optical coherence tomography reflective drusen substructures predict progression to geographic atrophy in age-related macular degeneration. *Ophthalmology*. 2016;123(12):2554–2570.
10. Oishi A, Thiele S, Nadal J, et al. Prevalence, natural course, and prognostic role of refractile drusen in age-related macular degeneration. *Invest Ophthalmol Vis Sci*. 2017;58(4): 2198–2206.
11. Li M, Dolz-Marco R, Huisingh C, et al. Clinicopathologic correlation of geographic atrophy secondary to age-related macular degeneration. *Retina*. 2019;39(4):802–816.
12. Jaffe GJ, Chakravarthy U, Freund KB, et al. Imaging features associated with progression to geographic atrophy in age-related macular degeneration: Classification of Atrophy Meeting report 5. *Ophthalmol Retina*. 2021;5(9): 855–867.
13. Sadda SR, Guymer R, Holz FG, et al. Consensus definition for atrophy associated with age-related macular degeneration on OCT: Classification of Atrophy report 3. *Ophthalmology*. 2018;125(4):537–548.
14. Guymer RH, Wu Z, Hodgson LAB, et al. Subthreshold nanosecond laser intervention in age-related macular degeneration: the LEAD randomized controlled clinical trial. *Ophthalmology*. 2019;126(6):829–838.
15. Steinle NC, Pearce I, Monés J, et al. Impact of baseline characteristics on geographic atrophy progression in the FILLY trial evaluating the complement C3 inhibitor pegcetacoplan. *Am J Ophthalmol*. 2021;227:116–124.

16. Jaffe GJ, Westby K, Csaky KG, et al. C5 inhibitor avacincaptad pegol for geographic atrophy due to age-related macular degeneration: a randomized pivotal phase 2/3 trial. *Ophthalmology*. 2021;128(4):576−586.
17. Holz FG, Sadda SR, Staurenghi G, et al. Imaging protocols in clinical studies in advanced age-related macular degeneration: recommendations from Classification of Atrophy Consensus Meetings. *Ophthalmology*. 2017;124(4):464−478.
18. Yehoshua Z, Rosenfeld PJ, Gregori G, et al. Progression of geographic atrophy in age-related macular degeneration imaged with spectral domain optical coherence tomography. *Ophthalmology*. 2011;118(4):679−686.
19. Yehoshua Z, Garcia Filho CA, Penha FM, et al. Comparison of geographic atrophy measurements from the OCT fundus image and the sub-RPE slab image. *Ophthalmic Surg Lasers Imaging Retina*. 2013;44(2):127−132.
20. Yehoshua Z, de Amorim Garcia Filho CA, Nunes RP, et al. Systemic complement inhibition with eculizumab for geographic atrophy in age-related macular degeneration: the COMPLETE study. *Ophthalmology*. 2014;121(3):693−701.
21. Yehoshua Z, de Amorim Garcia Filho CA, Nunes RP, et al. Association between growth of geographic atrophy and the complement factor I locus. *Ophthalmic Surg Lasers Imaging Retina*. 2015;46(7):772−774.
22. Schaal KB, Rosenfeld PJ, Gregori G, et al. Anatomic clinical trial endpoints for nonexudative age-related macular degeneration. *Ophthalmology*. 2016;123(5):1060−1079.
23. Schaal KB, Gregori G, Rosenfeld PJ. En face optical coherence tomography imaging for the detection of nascent geographic atrophy. *Am J Ophthalmol*. 2017;174:145−154.
24. Shi Y, Zhang Q, Zhou H, et al. Correlations between choriocapillaris and choroidal measurements and the growth of geographic atrophy using swept source OCT imaging. *Am J Ophthalmol*. 2021;224:321−331.
25. Shi Y, Yang J, Feuer W, et al. Persistent hypertransmission defects on en face OCT imaging as a stand-alone precursor for the future formation of geographic atrophy. *Ophthalmol Retina*. 2021;5(12):1214−1225.
26. Laiginhas R, Shi Y, Shen M, et al. Persistent hypertransmission defects detected on en face swept source OCT images predict the formation of geographic atrophy in AMD. *Am J Ophthalmol*. 2022;237:58−70.
27. Liu J, Laiginhas R, Corvi F, et al. Diagnosing persistent hyper-transmission defects on en face OCT imaging of age-related macular degeneration. *Ophthalmol Retina*. 2022; S2468-6530(22)00033-1. https://doi.org/10.1016/j.oret.2022.01.011. Online ahead of print.
28. Laiginhas R, Liu J, Shen M, et al. Multimodal imaging, OCT B-scan localization, and en face OCT detection of macular hyperpigmentation in eyes with intermediate age-related macular degeneration. *Ophthalmol Sci*. 2022;2(2):100116.
29. Jiang X, Shen M, Wang L, et al. Validation of a novel automated algorithm to measure drusen volume and area using swept source optical coherence tomography angiography. *Transl Vis Sci Technol*. 2021;10(4):11.
30. Goh KL, Abbott CJ, Hadoux X, et al. Hyporeflective cores within drusen: association with progression of age-related macular degeneration and impact on visual sensitivity. *Ophthalmol Retina*. 2022;6(4):284−290.
31. Lei J, Balasubramanian S, Abdelfattah NS, et al. Proposal of a simple optical coherence tomography-based scoring system for progression of age-related macular degeneration. *Graefes Arch Clin Exp Ophthalmol*. 2017;255(8):1551−1558.
32. Nassisi M, Lei J, Abdelfattah NS, et al. OCT risk factors for development of late age-related macular degeneration in the fellow eyes of patients enrolled in the HARBOR study. *Ophthalmology*. 2019;126(12):1667−1674.
33. Mullins RF, Johnson MN, Faidley EA, et al. Choriocapillaris vascular dropout related to density of drusen in human eyes with early age-related macular degeneration. *Invest Ophthalmol Vis Sci*. 2011;52(3):1606−1612.
34. Moult EM, Waheed NK, Novais EA, et al. Swept-source optical coherence tomography angiography reveals choriocapillaris alterations in eyes with nascent geographic atrophy and drusen-associated geographic atrophy. *Retina*. 2016;36(Suppl 1):S2−S11.
35. Nassisi M, Tepelus T, Nittala MG, Sadda SR. Choriocapillaris flow impairment predicts the development and enlargement of drusen. *Graefes Arch Clin Exp Ophthalmol*. 2019;257(10):2079−2085.
36. Lutty GA, McLeod DS, Bhutto IA, et al. Choriocapillaris dropout in early age-related macular degeneration. *Exp Eye Res*. 2020;192:107939.
37. Byon I, Ji Y, Alagorie AR, et al. Topographic assessment of choriocapillaris flow deficits in the intermediate age-related macular degeneration eyes with hyporeflective cores inside drusen. *Retina*. 2021;41(2):393−401.